Toxicology and Applied Pharmacology 288 (2015) 322–329

Contents lists available at ScienceDirect

Toxicology and Applied Pharmacology

journal homepage: www.elsevier.com/locate/ytaap

MyD88 mediates in vivo effector functions of alveolar macrophages in acute lung inflammatory responses to carbon nanotube exposure

Evan A. Frank [a], M. Eileen Birch [b], Jagjit S. Yadav [a,*]

[a] Division of Environmental Genetics and Molecular Toxicology, Department of Environmental Health, University of Cincinnati College of Medicine, Cincinnati, OH 45267, USA
[b] National Institute for Occupational Safety and Health, Cincinnati, OH 45213, USA

ARTICLE INFO

Article history:
Received 23 April 2015
Revised 23 July 2015
Accepted 7 August 2015
Available online 10 August 2015

Keywords:
Nanotoxicology
Particle toxicology
Molecular toxicology
Carbon nanotubes
Macrophage depletion

ABSTRACT

Carbon nanotubes (CNTs) are rapidly emerging as high-priority occupational toxicants. CNT powders contain fibrous particles that aerosolize readily in places of manufacture and handling, posing an inhalation risk for workers. Studies using animal models indicate that lung exposure to CNTs causes prolonged inflammatory responses and diffuse alveolar injury. The mechanisms governing CNT-induced lung inflammation are not fully understood but have been suggested to involve alveolar macrophages (AMs). In the current study, we sought to systematically assess the effector role of AMs in vivo in the induction of lung inflammatory responses to CNT exposures and investigate their cell type-specific mechanisms. Multi-wall CNTs characterized for various physicochemical attributes were used as the CNT type. Using an AM-specific depletion and repopulation approach in a mouse model, we unambiguously demonstrated that AMs are major effector cells necessary for the in vivo elaboration of CNT-induced lung inflammation. We further investigated in vitro AM responses and identified molecular targets which proved critical to pro-inflammatory responses in this model, namely MyD88 as well as MAPKs and Ca^{2+}/CamKII. We further demonstrated that MyD88 inhibition in donor AMs abrogated their capacity to reconstitute CNT-induced inflammation when adoptively transferred into AM-depleted mice. Taken together, this is the first in vivo demonstration that AMs act as critical effector cell types in CNT-induced lung inflammation and that MyD88 is required for this in vivo effector function. AMs and their cell type-specific mechanisms may therefore represent potential targets for future therapeutic intervention of CNT-related lung injury.

Introduction

Carbon nanomaterials are being applied to a rapidly growing number of biomedical, industrial, and engineering technologies. In particular, carbon nanotubes (CNTs) have been at the forefront of the material industry owing to their utility in numerous applications. These include use in advanced polymer composites and construction materials, cabling, heat shielding, and other applications in electrical and biotechnology systems (De Volder et al., 2013). Because of the nature of these uses and their ubiquitous need, the global prevalence of CNTs has grown rapidly and increases in their manufacture, transport, and processing are expected to continue for many years. Accordingly, the risk of human exposure to CNTs in occupational settings and the environment is expected to increase. CNTs can become airborne when manufactured or subsequently agitated and can persist as aerosols (Dahm et al., 2012; Han et al., 2008). CNTs must therefore be considered in terms of their potential as inhalational toxicants.

Published studies indicate that CNT exposures induce inflammatory features in animal models of acute lung exposure, including leukocytic infiltration and elaboration of pro-inflammatory cytokines and chemokines (Ma-Hock et al., 2009; Muller et al., 2008; Nygaard et al., 2009; Porter et al., 2010). Chronic exposure studies (Mercer et al., 2011; Wang et al., 2011) suggest that these effects lead to chronic pathologies such as hyperplasia and granulomatous lesions. Although descriptive toxicology studies have become widespread, much remains to be done concerning CNT toxicity mechanisms. There has been growing evidence of inflammasome activation by CNTs in various cell types (Hussain et al., 2014; Palomäki et al., 2011), and IL-1R signaling has been shown to be critical in acute inflammatory responses to exposure (Girtsman et al., 2014). However, many studies rely primarily on in vitro models or global knock-out mutants and thus may be limited in appreciating the complex orchestrations of in vivo toxic responses, which may involve the coordinated participation of specific effector cell compartments and cell type-specific mechanisms. This investigation was specifically aimed at identifying critical effector cells in the lung in vivo and the cellular and molecular mechanisms necessary for their

* Corresponding author at: University of Cincinnati College of Medicine, Department of Environmental Health, Kettering Laboratory Complex, 160 Panzeca Way, Cincinnati, OH 45267, USA.
E-mail address: Jagjit.Yadav@uc.edu (J.S. Yadav).

http://dx.doi.org/10.1016/j.taap.2015.08.004
0041-008X/

role as such. The objective is to help establish a mechanistic knowledge-base that may lend critical support to the development of therapeutic intervention strategies for potential CNT exposure-associated lung diseases.

Several published studies have observed that macrophages are activated and produce cytokines when exposed to CNTs in culture systems (Brown et al., 2007; Cheng et al., 2009; Hirano et al., 2008). In the lung, alveolar macrophages (AMs) are resident phagocytes localized in the bronchoalveolar spaces and airways. Their phenotype is distinct from those found in other locations such as the peritoneum and lung interstitium. The primary roles of AMs are maintaining immunological homeostasis of the terminal airspaces (Thepen et al., 1989) and the clearance of debris from the bronchoalveolar areas (Lehnert et al., 1989). AMs can mediate lung inflammation through the production of immunological mediators such as TNF, IL-1ß, and IL-6, which can increase capillary leakage, recruit inflammatory leukocytes, and promote the formation of granulomatous and fibrotic lesions (Ware, 2006; Marshall et al., 1996). The functions of AMs are necessary for the health of the lung, but they may also act to damage the organ when inflammatory responses are too severe or do not resolve appropriately (Oberdörster et al., 1992). Based on these observations, it is reasonable to hypothesize that AMs act as specific effector cells in lung responses to CNT exposures. However, this hypothesis has not been systematically tested in vivo.

We employed a selective, in vivo, cell-specific depletion and repopulation approach in a mouse model to assess the in vivo effector function of AMs and investigate underlying mechanistic events responsible for the inflammatory responses to CNT exposure in conjunction with an in vitro cell model.

Methods and materials

Reagents and chemicals

For routine work, phosphate-buffered saline (PBS) buffer and RPMI 1640 base medium were obtained from Hyclone through ThermoFisher (Waltham, MA). Fetal bovine serum (FBS) used was from Atlanta Biologicals (Flowery Branch, GA). For AM depletions, liposomal clodronate (LC) was obtained from Encapsula Nanosciences (Nashville, TN). For cytokine measurements, IL-1ß was measured using Duoset ELISA (R&D, Minneapolis, MN) and all other cytokines were measured using Ready-Set-Go ELISA (eBioscience, San Diego, CA). The following drugs were used for targeted inhibition studies: SB203580 (Tocris, Bristol, UK) for p38, SP600125 (Millipore, Billerica, MA) for JNK, pepinh-MYD (Invivogen, San Diego, CA) for MyD88.

CNT material preparation and characterization

High-purity multi-wall carbon nanotubes (MWCNTs, referred to as CNTs throughout this manuscript), produced using chemical vapor deposition, were obtained from Baytubes (Leverkusen, Germany) as a dry bulk powder form. Briefly, the material was characterized using the following analyses: size and morphology using scanning electron microscopy, metal content using inductively coupled plasma with atomic emission spectroscopy, surface area using the Brunauer, Emmett, and Teller (BET) method, and thermogravimetric analysis. Detailed description of the methods for material characterization analyses are given in supplementary information (SI).

To prepare our exposure-ready material, CNT powder was weighed and suspended in an appropriate aqueous delivery medium, using PBS buffer (for animal exposures) or RPMI medium base with no added FBS and antibiotics (for in vitro cell exposures). Pluronic F127 (Sigma, St. Louis, MO) was added (1% final concentration) in both cases to aid dispersion. Suspensions were subjected to ultrasonication for up to 2 h until dispersed suspensions were observed by microscopy. Suspensions were centrifuged (3200g for 30 min) to pellet large CNT aggregates, and pellets were dried and weighed to determine the suspension concentrations. LAL Chromogenic Endotoxin Assay (Pierce, Rockford, IL) was used to screen for potential contaminating endotoxin, which was not detected in cleared supernatants. For visualization of the particles, transmission electron microscopy (TEM) was performed (see SI for method). Sizes of imaged CNTs were measured using ImageJ software (http://imagej.nih.gov). The suspended sample was also subjected to elemental carbon analysis using a thermal–optical analyzer described previously (Birch and Cary, 1996; Birch, 2004a,b) and in SI.

Animal exposures

The use of animals in this study was approved by the University of Cincinnati Institutional Animal Care and Use Committee, Cincinnati, Ohio 45221, USA. For routine experiments, 6 week-old CF-1 Non-Swiss Albino mice were purchased from Harlan Laboratory (Haslett, MI). All experiments used an $n = 4$. To administer exposures via orotracheal aspiration, animals were anesthetized with isoflurane and suspended on an inclined plane. The tongue was held and a 50-μL bolus was placed at the back of the tongue. The nose was held until the animal had fully aspirated the bolus and drawn two deep recovery breaths. Animals were exposed to 4 mg/kg body weight CNTs for experiments, which translated to 0.774 m^2 CNT surface area per kg body weight based on CNT surface area analysis (see Results). The same aspiration technique was used for AM depletion or adoptive transfer/reconstitution experiments. For depletion of AMs, 70 μL of 5 mg/mL LC was administered to the lung 8–24 h prior to experimental exposures. To reconstitute AMs by adoptive transfer, naïve CF-1 mice were euthanized and exsanguinated. Bronchoalveolar lavage (BAL) was performed and AMs (>99% purity based on morphology) were collected by centrifugation. Donor AMs (1×10^5 AMs/mouse) were immediately instilled via aspiration into AM-depleted mice (20 h after LC administration), 1 h prior to CNT exposures. To assess the dependence of in vivo responses on MyD88, donor AMs were incubated for 2 h in complete cell culture media with 100 μM pepinh-MYD peptide before being instilled as above. Control donor AMs were incubated with no peptide inhibitor.

Determination of lung cells and cytokines

Animals were sacrificed by 20-μL IP injection of Euthasol (Butler Schein, Dublin, OH). Exsanguination was performed by severing the vena cava. BAL was performed by exposing and canulating the trachea and two 1-mL lavages of PBS were performed. Lavage cells were centrifuged and cytokines were measured in the supernatants using ELISA. Cells from BAL fluid were resuspended in PBS/5% FBS for total cell counting. Differential cell counts were obtained using cytospin centrifugation followed by Hema3 staining to type cells based on morphology. Differences among groups were evaluated for significance using one-way ANOVA with Tukey post-hoc analysis.

Cell culture and in vitro experiments

In vitro macrophage responses were tested using the murine alveolar macrophage cell line MH-S (ATCC, Manassas, VA). Cells were cultured in complete RPMI1640 medium at 37 °C in a 5% CO_2 incubator. For experiments, cells were seeded at 5×10^5 cells/mL with $n = 4$ (replicate wells) and the medium was supplemented with vehicle or CNT preparation (400 μg/mL final concentration) for selected durations. The in vitro exposure dose was chosen based on dose–response curves (shown in SI) and this dose translated to a CNT surface area of 77.4 cm^2/mL in culture media. To measure cytokine production, supernatants were collected and centrifuged to remove suspended cells. Pelleted cells were combined with monolayer and lysed in non-denaturing lysis buffer (20-mM Tris–HCl, 150-mM NaCl, 1-mM EDTA, 1% Triton X-100). Cytokines were measured in the culture supernatant (TNF) or cell lysate (IL-1ß) as above. For pathway inhibition studies, respective inhibitory agents were added to the culture medium 1 h prior to CNT exposure.

Significant differences in levels of cytokines versus control were evaluated using one-way ANOVA with Dunnett's test for multiple one-sided comparisons.

Results

Physicochemical characterization of CNTs

SEM of 'as-supplied' CNTs showed that dry bulk particles were composed of compact aggregates. The size distribution of dry, unprocessed aggregate particles is given in Fig. S1. Average metal contents ($n = 3$) and TGA results are shown in Table 1. The following metals were found in decreasing content order: Co, Mn, Mg, Al, and Ni. The results of thermogravimetric analysis ($n = 3$) indicated a peak decomposition temperature of 598 °C. The average surface area of CNTs, determined by duplicate BET analysis, was 193.6 m^2/g, with a relative percent difference of 0.9.

TEM showed that 'as-instilled' CNT materials in suspension were primarily composed of loose, tangled agglomerates (Fig. 1). Occasionally, isolated CNT fibers (not shown) also were observed. The mean CNT diameter was 10.7 ± 3.1 nm. It was not possible to accurately measure length but the majority of fibers appeared to be 1 μm or longer. In comparing the elemental carbon and CNT mass concentrations of the suspensions, a test concentration of 660 μg/mL CNTs was measured to be 664 ± 15 μg/mL elemental carbon.

CNT exposure induced acute neutrophilic inflammation in the lung

Exposure to CNTs (4 mg/kg body weight) in adult mice ($n = 4$) via orotracheal aspiration caused a time-dependent inflammation in the lung as measured by the quantification of neutrophils and pro-inflammatory mediators in bronchoalveolar lavage (BAL) fluid collected at selected time points (Fig. 2). Neutrophilia peaked at 24 h post-exposure, declining to above-baseline levels in the following days. Cells found in BAL fluid consisted almost exclusively of macrophages and neutrophils. The number of macrophages did not change appreciably in the time period examined. Vehicle controls were performed with $n = 3$ at 24, 48, and 72 h and showed no signs of neutrophilic inflammation or any other change, and are not shown. TNFα and IL-6 cytokines increased following CNT exposure, peaking at 6 h post-exposure and declining thereafter. Cytokine levels in above vehicle controls were negligible and an average of the controls is shown as a background reference. These data indicate that CNT exposures cause an acute inflammatory reaction in the lung consisting primarily of neutrophilic infiltration.

Table 1
Metal content (top) and thermogravimetric analysis (bottom) of carbon nanotubes.

Element	Average μg/mg	STD	Error
Co	2.7545	0.1752	.0636
Mn	2.5123	0.1158	.0461
Mg	2.0892	0.1842	.0882
Al	1.9245	0.1308	.068
Ni	.0631	0.0018	0.029

Sample	IDT[a] °C	PDT[b] °C	EDT[c] °C	RW[d] %
CNT	502	598	675	2

[a] ,Initial decomposition temperature, weight loss > 5%.
[b] ,Peak decomposition temperature.
[c] ,Ending decomposition temperature, weight change < 0.1%/min.
[d] ,Residual weight.

AM depletion attenuated CNT-induced inflammation in the lung

AM depletion via orotracheal administration of liposomal clodronate (LC) 8 h prior to CNT exposure attenuated the influx of neutrophils (Fig. 3). The greatest difference was seen at the peak of inflammation 24 h after exposure. The number of neutrophils recovered from LC-pretreated mice at this time point was reduced to 49 ± 17% of that from animals treated with CNT alone. For reproducibility, this experiment was repeated at the 24 h time point and the results are presented pooled. It should be noted that liposomal suspensions alone also induce some neutrophilic infiltration in lungs. In this context, a control experiment showed that pre-treatment with blank (non-LC) liposomes (obtained from the same vendor) prior to CNT exposure resulted in increased neutrophil count compared to CNT exposures alone (Fig. S2), thus the attenuated CNT-induced neutrophilia following LC treatment was attributed to depletion of AMs. Pretreatment of mice with LC also sharply attenuated levels of pro-inflammatory cytokines induced by CNT exposure (Fig. 4); TNF and IL-6 levels were decreased to 42 ± 19% and 10 ± 33%, respectively. As above, these results were confirmed in a repeat experiment and the data are presented as an average. Collectively, the above observations indicated that depletion of AMs by LC pretreatment attenuates inflammation caused by acute CNT exposures.

AM reconstitution rescued lung inflammatory response to CNTs

We sought to confirm the specific role of AMs as effector cells in CNT-induced inflammatory endpoints by testing whether reconstitution of the AM population by adoptive transfer from naïve donor mice into the AM-depleted mice prior to CNT exposure could rescue inflammatory responses. In this experiment, the group exposed to CNTs alone is used as the baseline (100% of neutrophilic response). Macrophage depletion via 18 h pretreatment with LC significantly attenuated neutrophilia (measured in BAL fluid) to 44.6 ± 14.7% of baseline, as in the previous experiment. Reintroduction of AMs 1 h prior to exposure rescued this endpoint to 75.6 ± 5.6% of baseline (Fig. 5). Reintroduction of AMs without subsequent CNT exposure had no apparent difference from the LC + CNT group. In addition, CNT-induced pro-inflammatory cytokines were recovered by AM reintroduction (Fig. 6). TNF attenuated by AM depletion recovered partially by reintroduction of AMs (44.2 ± 14.9% in LC + CNT to 79.4 ± 5.5% in LC + AM + CNT). IL-6 in the LC + AM + CNT group was increased relative to groups not exposed to CNTs, but not relative to the LC + CNT group, suggesting that this cytokine may not play as influential a role as TNF in determining the extent of neutrophilic inflammation in this case. These data suggest that the presence of AMs is a determining factor in the ability of LC-mediated AM depletion to stunt CNT-induced inflammatory responses and demonstrate that AMs are critical effector cells in the full elaboration of CNT-induced acute inflammation.

CNT-induced cytokine production by AMs is partially dependent on MAP kinases p38 and JNK

MH-S cells pre-incubated with inhibitors for p38 and JNK pathways exhibited blunted production of TNF and IL-1ß compared to naïve cells (Fig. 7) following in vitro exposure to 400 μg/mL CNTs. This dose was determined by dose–response data shown in Fig. S3. p38 inhibition reduced levels of both TNF and IL-1ß, whereas JNK inhibition reduced levels of TNF but did not affect IL-1ß. The data demonstrate that full elaboration of CNT-induced TNF and IL-1ß by AMs is dependent on p38 and JNK pathways.

Cytokine induction in AMs is dependent on calcium- and MyD88-signaling

A series of drug-based inhibition studies indicated two critical mechanisms of CNT-induced AM responses in this study (Fig. 8).

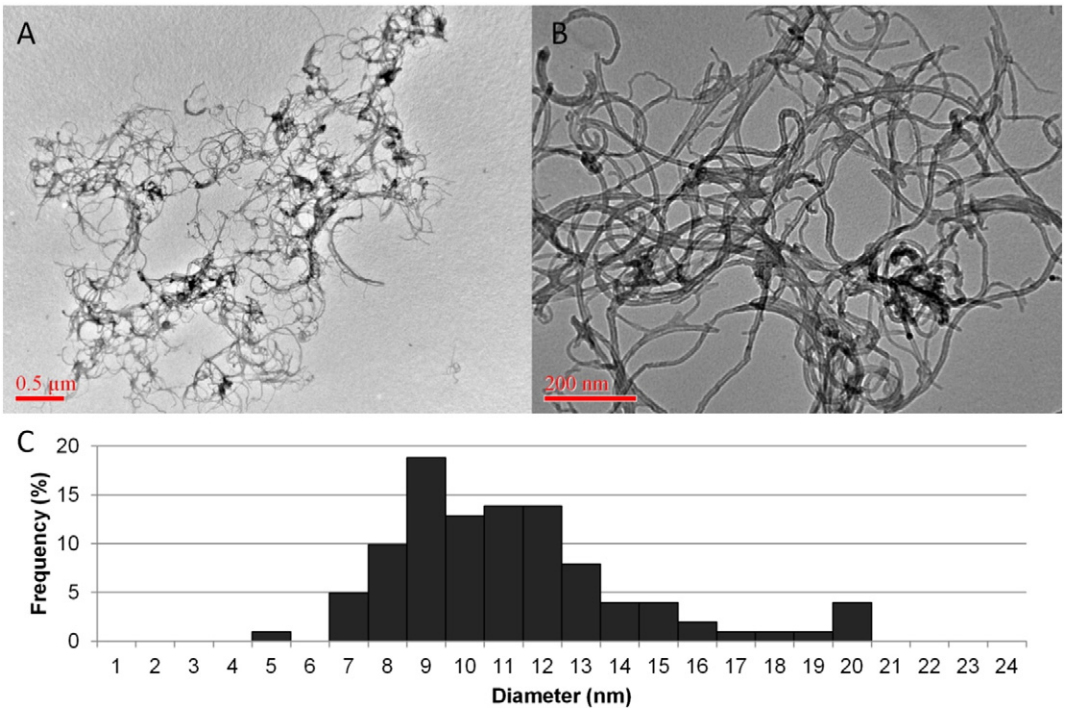

Fig. 1. TEM characterization of CNTs used in this study. TEM micrographs were used to characterize physical dimensions of CNTs following preparation in aqueous delivery medium. A: Low magnification, B: higher magnification, C: frequency distribution of CNT diameter. Measured diameters yielded the following statistics (in nm): mean = 10.7; SD = 3.1; Q1 = 8.6; Q3 = 11.9; min = 4.9; max = 19.9.

Chlorpromazine, a drug which perturbs Ca^{+}-dependent activity, nearly fully abrogated production of both TNF and IL-1ß. Pretreatment with pepinh-MYD inhibitory peptide specific for MyD88 completely abolished both TNF and IL-1ß induced by CNT exposure, indicating that AMs require this pathway to produce these cytokines in direct response to CNT exposure.

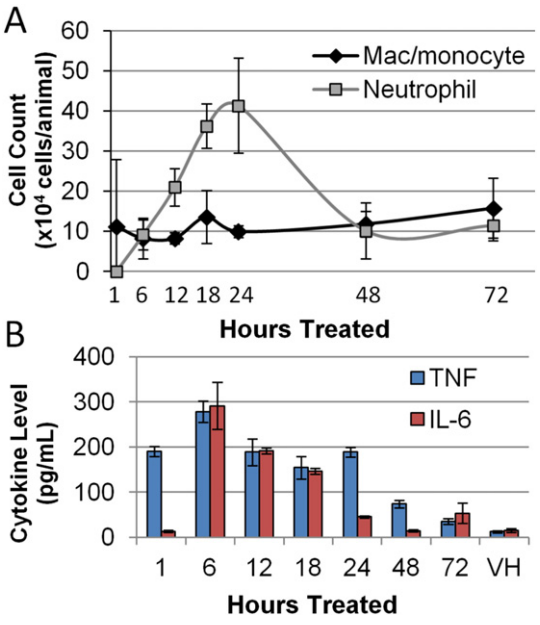

Fig. 2. CNT exposures caused acute neutrophilic inflammation in the lung in a mouse model. NSA mice ($n = 4$) received 4 mg/kg CNT or vehicle at t = 0 and sampled over 72 h. BAL fluid was collected at time points shown and cells were counted by type (A). Vehicle controls (not shown) performed at 24, 48, and 72 h showed no signs of inflammation in neutrophilia or cytokines. Cytokines were measured using ELISA (B) and an average of 24, 48, and 72 h vehicle controls is shown (VH) for background reference.

MyD88 function is required for AM-dependent inflammatory responses to CNT exposures in vivo

Based on the in vitro observations, we hypothesized that MyD88 inhibition in AMs would decrease their effectiveness as effector cells of CNT-induced inflammatory responses in vivo. We used a variation of the adoptive transfer model in which donor AMs from naïve mice were incubated for 2 h with or without MyD88 inhibitory peptide. Again using a CNT-only control as a baseline 100% response, transfer of control AMs incubated for 2 h with no peptide into AM-depleted mice reproduced the aforementioned results, showing a 76.4 ± 6.5% response when neutrophilia was measured. Transfer of MyD88-inhibited AMs in the same case resulted in 43.1 ± 4% of the measured response, indistinguishable from the AM depletion-mediated attenuation of neutrophilia characterized in earlier experiments (Fig. 9), and significantly less than the level seen with transfer of naïve AMs. Similarly, MyD88-inhibited AMs failed to rescue CNT-induced TNF and IL-6 as

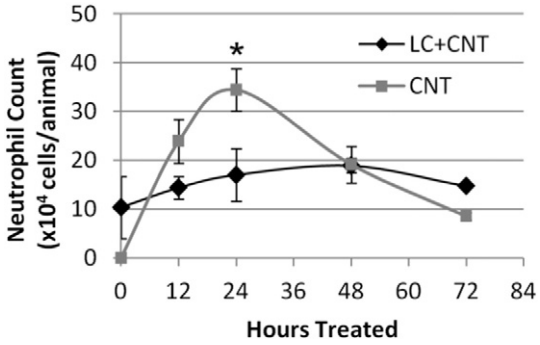

Fig. 3. Depletion of AMs attenuated neutrophilic inflammation of the lung in a mouse model of CNT exposure. Neutrophils were quantified in BAL fluid collected at indicated time points following exposure to CNTs (4 mg/kg). Peak neutrophilia induced by CNT exposure (at 24 h) was reduced to 49% ± 17 in animals which received an AM-depleting dose of LC (LC + CNT) prior to exposure. $n = 4$, *$p < 0.05$.

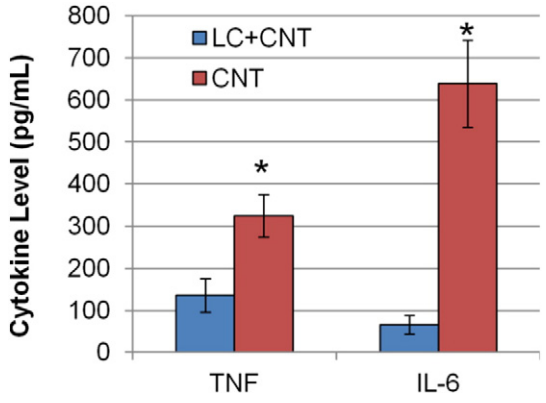

Fig. 4. Depletion of AMs attenuated levels of CNT-induced cytokines in the lung in a mouse model. TNF and IL-6 were measured in BAL fluid collected 12 h following CNT exposure. Both cytokines were decreased in animals which received an AM-depleting dose of LC prior to exposure. $n = 4$, *$p < 0.05$.

measured in BAL fluid. Both TNF and IL-6 were rescued by naïve AMs in this experiment (Fig. 10), in contrast to earlier observations (Fig. 6) in which AM transfer rescued TNF only. This difference may be due to the 2 h incubation interval, which may improve the competency of transferred AMs to produce and/or elicit IL-6 in this model.

Discussion

While toxicological studies continue to make progress in the characterization of toxic lung responses to CNT exposures, more remains to be done to identify critical mechanisms which could potentially serve as targets for therapeutic intervention. We have approached this knowledge gap by first seeking to demonstrate critical effector cells of toxic responses in the lung and then investigating their molecular mechanisms. We have used this approach to identify effector cell-specific mechanisms of CNT toxicity through systematic experimentation in an in vivo exposure model.

Because of their short history of manufacture and use, there is no confirmed reference for the amount of accumulated inhaled CNT

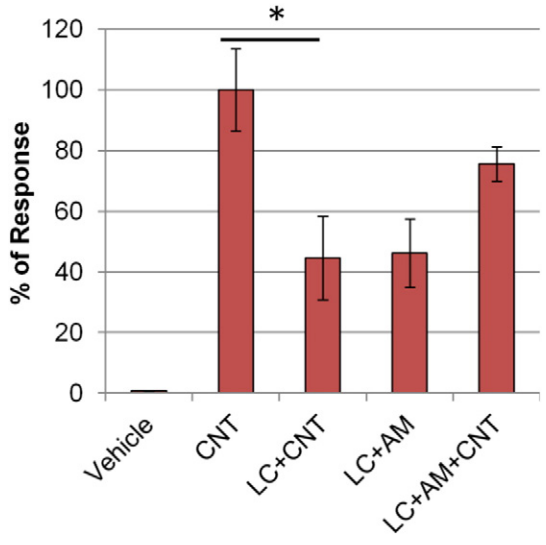

Fig. 5. Reintroduction of AMs rescued CNT-induced neutrophilic response in the lung of a mouse model of CNT exposure. Values are expressed here as percentage of baseline neutrophilic response (CNT). Macrophage depletion here (LC + CNT) attenuated the response to 44.6 ± 14.7% (of CNT alone). Adoptive transfer of AMs into macrophage-depleted animals (LC + AM + CNT) resulted in partial rescue of CNT-induced neutrophils (75.6 ± 5.6% of CNT alone). Reintroduction of AMs without subsequent CNT exposure (LC + AM) had no observed effect. $n = 4$, *$p < 0.05$.

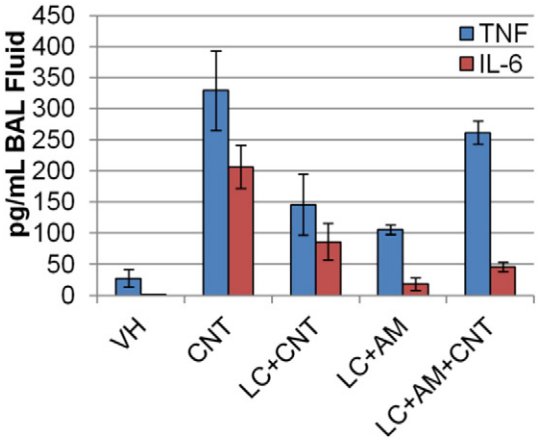

Fig. 6. Effect of reintroduction of AMs on CNT-induced pro-inflammatory cytokines in the lung of a mouse model of CNT exposure. Adoptive transfer of AMs into macrophage-depleted animals (LC + AM + CNT) resulted in partial rescue of CNT-induced TNF (44.2 ± 14.9% in LC + CNT to 79.4 ± 5.5% in LC + AM + CNT) as measured in BAL fluid in a manner which mirrored the effect on neutrophilia. $n = 4$.

material expected during a realistic occupational lifetime which would guide relevant dosing in experimental models. We therefore designed our initial studies based on our preliminary dose–response analysis in mice indicating 4 mg/kg CNTs as scientifically appropriate to pursue mechanistic experiments. Furthermore, this dose approximates those used in several important published studies (Mercer et al., 2011; Nygaard et al., 2009; Porter et al., 2010), which will aid interpretation of this work in the context of existing and ongoing efforts in this field.

The strategy employed here for assessing the role of AMs in exposure-related lung responses involved depleting these cells from the lung using instillation of liposomal clodronate, in which a cytotoxic drug is encapsulated in liposomes which are selectively taken up by AMs. This approach has been successfully used for other lung

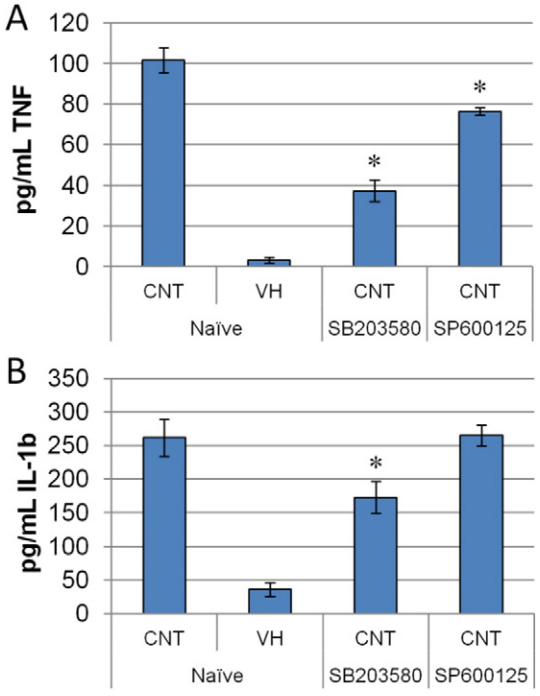

Fig. 7. Cytokine induction in AMs (MH-S cells) following CNT exposure is partially dependent on the MAP kinases p38 and JNK. TNF production by AMs was significantly reduced (A) by pre-incubation with 20 μM of p38 inhibitor SB203580 or JNK inhibitor SP600125. Pre-incubation with 20 μM p38 inhibitor significantly reduced IL-1ß production (B); JNK inhibition had no effect. $n = 4$, *$p < 0.05$.

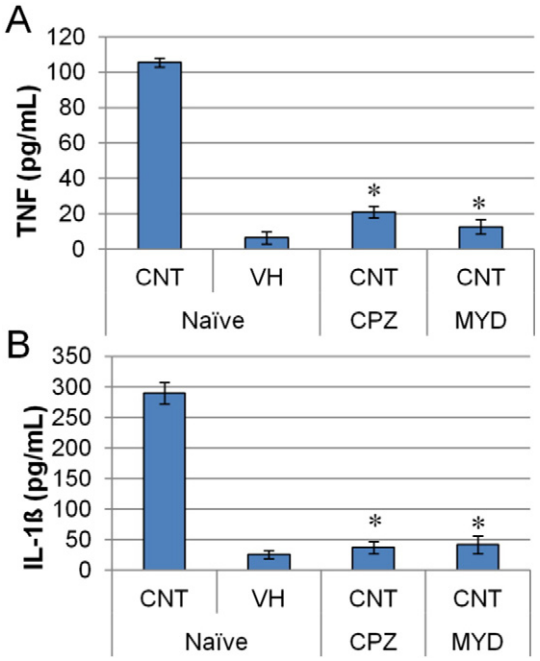

Fig. 8. CNT-induced TNFα and IL-1ß production in AMs (MH-S cells) is dependent on calcium- and MyD88-signaling. Pretreatment with drugs chlorpromazine (CPZ, 20 μM) or inhibitory peptide pepinh-MYD (MYD, 100 μM) were used to inhibit calcium signaling and MyD88 signaling, respectively. Both drugs abrogated production of TNF (A) and IL-1ß (B). $n = 4$, $p < 0.05$.

pathogenesis models including studies on control of influenza (Tate et al., 2010) and Pseudomonas (Kooguchi et al., 1998) infections as well as various mechanisms of injury including ischemia–reperfusion (Zhao et al., 2006) and ventilator-induced injury (Frank et al., 2006). However, to our knowledge, this approach has not been reported for nanotoxicology studies. In our studies, AM depletion regularly reduced CNT-induced neutrophilic inflammation by ~50%. This indicates a significant effector role for AMs, although the attenuation of the effect is not total. Two reasons may account for this: first, AM depletion by LC is not total. We routinely measured AMs in the BAL fluid of LC-treated animals in the range of 22–50% of the number retrieved from control

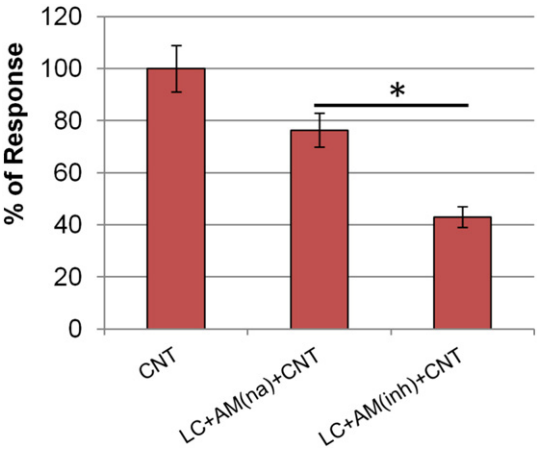

Fig. 9. Inhibition of MyD88 in primary AMs transferred into AM-depleted mice led to no rescue of CNT-induced neutrophilia. Values are expressed here as percentage of baseline neutrophilic response (CNT). Adoptive transfer of AMs (10^5/animal) treated with MyD88 inhibitory peptide (2 h pre-incubation) into macrophage-depleted animals (LC + AM(inh) + CNT) resulted in no rescue of CNT-induced neutrophils (43.1 ± 4% of CNT alone), while normal rescue (76.4 ± 6.5% of CNT alone) was observed after reintroduction of AMs incubated without inhibitory peptide (LC + AM(na) + CNT). $n = 4$, $^*p < 0.05$.

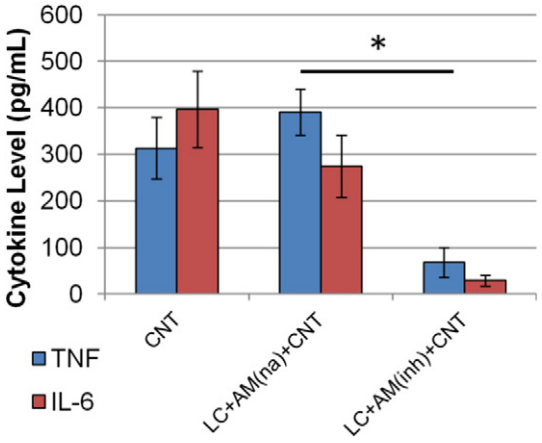

Fig. 10. Inhibition of MyD88 in primary AMs transferred into AM-depleted mice did not rescue CNT-induced proinflammatory cytokines. Adoptive transfer of AMs incubated with MyD88 inhibitory peptide into macrophage-depleted animals (LC + AM (inh) + CNT) resulted in no rescue of CNT-induced TNFα and IL-6, while robust rescue was observed in both endpoints after reintroduction of AMs incubated without inhibitory peptide (LC + AM (na) + CNT). $n = 4$, $^*p < 0.05$.

animals. That the attenuation of inflammation is partial may simply reflect partial nature of the depletion, with remaining AMs still capable of mounting a partial response. Second, AMs may not be the only cell population with effector functions in this scenario. Epithelial cells, for example, may contribute directly to the elicitation of in vivo lung responses to CNT exposures. Furthermore, mast cells have been shown to act as effector cells for selected lung responses to exposure (Katwa et al., 2012). These considerations motivated our need to confirm the effector role of AMs using adoptive transfer models.

Numerous studies have highlighted the direct effects of in vitro CNT exposures on macrophage-like cells in the form of both cell lines and primary cells and generally report similar responses including production of pro-inflammatory cytokines, among other assorted effects (Cheng et al., 2009; Hirano et al., 2008; Hussain et al., 2014; Muller et al., 2008). At least one study (Hirano et al., 2008) reports in vitro responses of apparently similar magnitude shown here at considerably lower concentrations of CNTs by weight. We suggest that this variability arises primarily from differences in physicochemical characteristics between specific materials used in various studies. Physicochemical characterization showed that the CNTs used in our study carry negligible levels of contaminating metals and no detectable iron, which has been recognized to account for observed effects in some studies (Kagan et al., 2006; Pulskamp et al., 2007). In addition, diameters of CNTs in this study were between 5 and 20 nm, whereas many other published studies used larger diameter CNTs in the range of 60–80 nm (Brown et al., 2007; Hirano et al., 2008). CNTs of the larger diameter have a more needle-like quality and have been shown to cause damage through partial internalization or skewering of cells, which may or may not rely on cellular uptake processes (Hirano et al., 2008). Particles of the smaller diameter CNTs used in this study displayed a more curled, tangled morphology and may not exert such effects. In light of these considerations in addition to the many limitations of cell line-based models in this situation, we have limited our use of in vitro AM models in this study to the screening of inhibitory drugs where the use of primary AMs would not be economical due to their limited availability.

We demonstrate here a critical role for MyD88 in the AM-mediated inflammatory response to CNTs. This molecule was found to be critical for in vitro production of CNT-induced cytokines and was furthermore necessary for AM-mediated rescue of CNT-induced inflammation in vivo. All TLRs (except TLR3) and IL-1 receptors rely on this adapter molecule for signaling function (Trinchieri and Sher, 2007). As mentioned earlier, IL-1R is now known to play a role in the regulation of CNT-induced inflammation in vivo, thus the demonstrated importance

of AM-specific MyD88 may relate to such emerging findings. Meanwhile TLRs, including TLR4, are being shown to be involved in lung responses to an increasing number of insults beyond classical stimuli such as LPS (Li et al., 2011; Maes et al., 2006). The current study suggests a key role of the MyD88 pathway in mechanisms of CNT toxicity, which may involve IL-1R- or TLR-dependent signaling. As detailed in Fig. 11, a proposed scheme of MyD88-linked mechanisms of action could include perturbation of the cell membrane and receptor ligation (or clustering of trans-activating receptors). These events may cause receptor-linked MyD88 to act on downstream IRAKs and TRAFs which then induce pro-inflammatory NF-κB and AP-1 pathways. As supported by other studies (Hussain et al., 2014; Palomäki et al., 2011), internalized CNTs may also cause lysosomal instability and NLRP3 inflammasome activation, leading to production of mature IL-1 s and positive feedback through IL-1R, which may be MyD88-dependent. These proposed mechanisms may be relevant to cytokine expression seen in MyD88-dependent macrophage responses to other toxicants as well (Uto et al., 2011; Chang et al., 2013; Ho et al., 2013).

In vitro, MAPK inhibitors for p38 and JNK and Ca^{+2} antagonist significantly blocked AM responses to CNTs. This suggests a role for MAPK- and Ca^{2+}-signaling pathways in the elaboration of AM responses to CNTs. The protein kinases p38 and JNK are commonly responsive to stress, heat, osmotic shock and a variety of stress stimuli, including single-wall CNTs (Azad et al., 2013). These MAPKs also modulate signaling downstream of MyD88 by acting on AP-1 (Shaulian and Karin, 2002). Reports on involvement of MAPKs in toxic responses to MWCNTs present mixed outcomes (Hirano et al., 2008; Lee et al., 2012), which may be a result of physiochemical differences between CNTs. Further investigation into specific players in these signaling pathways may potentially uncover valuable targets for therapies against immune cell-mediated CNT toxicity. The Ca^{2+}/CamKII signaling axis is known to be implicated in the process of immune cell activation in response to pathogens, stress, and soluble mediators and AM-mediated inflammatory insults (Brown et al., 2004; Alkharfy et al., 2000). To our knowledge, this is the first observation on the role of this signaling in CNT toxicity. Furthermore, as chlorpromazine is known to inhibit clathrin-mediated endocytosis (Wang et al., 1993), the results suggest that AM responses may arise from CNTs internalized by this mechanism.

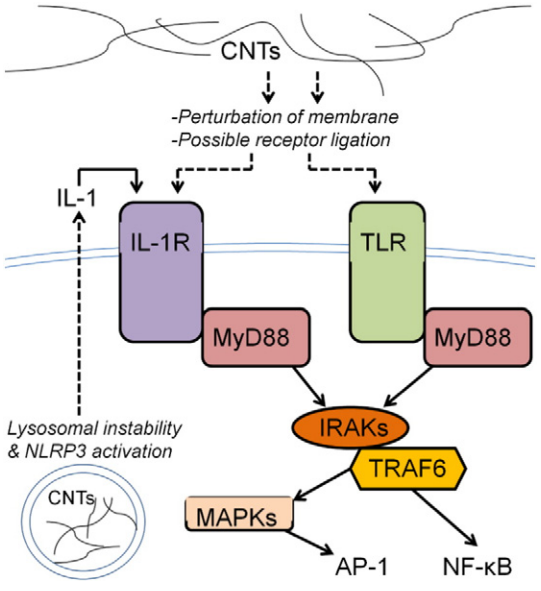

Fig. 11. Proposed role of MyD88 and MAPKs in the overall mechanism of action in AM responses to CNTs. MyD88 may link CNT exposures to inflammatory responses though IL-1-dependent feedback through IL-1R or activation of TLRs, with p38 and JNK MAPKs modulating downstream AP-1 activity. Known interactions in these pathways are shown by solid arrows. Proposed mechanisms of action by CNTs (dotted arrows) are based on the current and related studies (Girtsman et al., 2014; Hussain et al., 2014; Palomäki et al., 2011).

In conclusion, this work is the first to experimentally confirm in vivo that alveolar macrophages act as critical effector cells in CNT-related lung changes, and that MyD88 plays a crucial role in the functions of these effectors. These conclusions will serve to advance the knowledge of pathogenic mechanisms related to exposure to this important emerging class of occupational and environmental particle toxicants. Additionally, the strategy employed highlights the potential for effector cell-targeted intervention with minimal off-target effects in a therapeutic context.

Declaration of interest

The authors declare no conflicts of interest.

Transparency document

The Transparency document associated with this article can be found, in the online version.

Acknowledgments

The authors would like to acknowledge Dr. Marepalli B. Rao (University of Cincinnati) for his expert assistance in the selection and application of statistical methods in this study. This work was supported by the National Institutes of Health/National Institute for Environmental Health Sciences Center for Environmental Genetics (CEG) funds [2P30ES006096-16A1 to JSY], Gene-Environment Interactions Training Program (GEITP) fellowship [T32ES016646 to EAF], and National Institute of Occupational Safety and Health/Education and Research Center (ERC) funding [T42OH008432-07 to EAF], and the University of Cincinnati resources (to JSY).

Appendix A. Supplementary data

Supplementary data to this article can be found online at http://dx.doi.org/10.1016/j.taap.2015.08.004.

References

Alkharfy, K.M., Kellum, J.A., Matzke, G.R., 2000. Unintended immunomodulation: Part II. Effects of pharmacological agents on cytokine activity. Shock 13 (5), 346–360.
Azad, N., Iyer, A.K.V., Wang, L., Liu, Y., Lu, Y., Rojanasakul, Y., 2013. Reactive oxygen species-mediated p38 MAPK regulates carbon nanotube-induced fibrogenic and angiogenic responses. Nanotoxicology 7 (2), 157–168.
Birch, M.E., 2004a. Monitoring of diesel particulate exhaust in the workplace. In: Schlecht, P.C., O'Connor, P.F. (Eds.), NIOSH Manual of Analytical Methods (NMAM), 4th ed. Department of Health and Human Services, Public Health Service, Center for Disease Control and Prevention, National Institute for Occupational Safety and Health. DHHS(NIOSH):154, Cincinnati, Ohio.
Birch, M.E., 2004b. NIOSH method 5040 update. In: Schlecht, P.C., O'Connor, P.F. (Eds.), NIOSH Manual of Analytical Methods (NMAM), 4th ed. Third Supplement to NMAM. Department of Health and Human Services, Public Health Service, Center for Disease Control and Prevention, National Institute for Occupational Safety and Health. DHHS(NIOSH):154, Cincinnati, Ohio.
Birch, M.E., Cary, R.A., 1996. Elemental carbon-based method for monitoring occupational exposures to particulate diesel exhaust. Aerosol Sci. Technol. 25 (3), 221–241.
Brown, D.M., Donaldson, K., Borm, P.J., Schins, R.P., Dehnhardt, M., Gilmour, P., Jimenez, L.A., Stone, V., 2004. Calcium and ROS-mediated activation of transcription factors and TNF-α cytokine gene expression in macrophages exposed to ultrafine particles. Am. J. Physiol. Lung Cell. Mol. Physiol. 286 (2), L344–L353.
Brown, D.M., Kinloch, I.A., Bangert, U., Windle, A.H., Walter, D.M., Walker, G.S., Scotchford, C.A., Donaldson, K., Stone, V., 2007. An in vitro study of the potential of carbon nanotubes and nanofibres to induce inflammatory mediators and frustrated phagocytosis. Carbon 45 (9), 1743–1756.
Chang, H., Ho, C.C., Yang, C.S., Chang, W.H., Tsai, M.H., Tsai, H.T., Lin, P., 2013. Involvement of MyD88 in zinc oxide nanoparticle-induced lung inflammation. Exp. Toxicol. Pathol. 65 (6), 887–896.
Cheng, C., Müller, K.H., Koziol, K.K., Skepper, J.N., Midgley, P.A., Welland, M.E., Porter, A.E., 2009. Toxicity and imaging of multi-walled carbon nanotubes in human macrophage cells. Biomaterials 30 (25), 4152–4160.

Dahm, M.M., Evans, D.E., Schubauer-Berigan, M.K., Birch, M.E., Fernback, J.E., 2012. Occupational exposure assessment in carbon nanotube and nanofiber primary and secondary manufacturers. Ann. Occup. Hyg. 56 (5), 542–556.
De Volder, M.F., Tawfick, S.H., Baughman, R.H., Hart, A.J., 2013. Carbon nanotubes: present and future commercial applications. Science 339 (6119), 535–539.
Frank, J.A., Wray, C.M., McAuley, D.F., Schwendener, R., Matthay, M.A., 2006. Alveolar macrophages contribute to alveolar barrier dysfunction in ventilator-induced lung injury. Am. J. Physiol. Lung Cell. Mol. Physiol. 291 (6), L1191–L1198.
Girtsman, T.A., Beamer, C.A., Wu, N., Buford, M., Holian, A., 2014. IL-1R signaling is critical for regulation of multi-walled carbon nanotubes-induced acute lung inflammation in C57Bl/6 mice. Nanotoxicology 8 (1), 17–27.
Han, J.H., Lee, E.J., Lee, J.H., So, K.P., Lee, Y.H., Bae, G.N., Lee, S., Ji, J.H., Cho, M.H., Yu, I.J., 2008. Monitoring multiwalled carbon nanotube exposure in carbon nanotube research facility. Inhal. Toxicol. 20 (8), 741–749.
Hirano, S., Kanno, S., Furuyama, A., 2008. Multi-walled carbon nanotubes injure the plasma membrane of macrophages. Toxicol. Appl. Pharmacol. 232 (2), 244–251.
Ho, C.C., Luo, Y.H., Chuang, T.H., Yang, C.S., Ling, Y.C., Lin, P., 2013. Quantum dots induced monocyte chemotactic protein-1 expression via MyD88-dependent Toll-like receptor signaling pathways in macrophages. Toxicology 308, 1–9.
Hussain, S., Sangtian, S., Anderson, S.M., Snyder, R.J., Marshburn, J.D., Rice, A.B., Bonner, J.C., Garantziotis, S., 2014. Inflammasome activation in airway epithelial cells after multi-walled carbon nanotube exposure mediates a profibrotic response in lung fibroblasts. Part. Fibre Toxicol. 11 (1), 28.
Kagan, V.E., Tyurina, Y.Y., Tyurin, V.A., Konduru, N.V., Potapovich, A.I., Osipov, A.N., Kisin, E.R., Schwegler-Berry, D., Mercer, R., Castranova, V., Shvedova, A.A., 2006. Direct and indirect effects of single walled carbon nanotubes on RAW 264.7 macrophages: role of iron. Toxicol. Lett. 165 (1), 88–100.
Katwa, P., Wang, X., Urankar, R.N., Podila, R., Hilderbrand, S.C., Fick, R.B., Rao, A.M., Ke, P.C., Wingard, C.J., Brown, J.M., 2012. A carbon nanotube toxicity paradigm driven by mast cells and the IL-33/ST2 axis. Small 8 (18), 2904–2912.
Kooguchi, K., Hashimoto, S., Kobayashi, A., Kitamura, Y., Kudoh, I., Wiener-Kronish, J., Sawa, T., 1998. Role of alveolar macrophages in initiation and regulation of inflammation in pseudomonas aeruginosa pneumonia. Infect. Immun. 66 (7), 3164–3169.
Lee, J.K., Sayers, B.C., Chun, K.S., Lao, H.C., Shipley-Phillips, J.K., Bonner, J.C., Langenbach, R., 2012. Multi-walled carbon nanotubes induce COX-2 and iNOS expression via MAP Kinase-dependent and-independent mechanisms in mouse RAW264. 7 macrophages. Part. Fibre Toxicol. 9, 14.
Lehnert, B.E., Valdez, Y.E., Tietjen, G.L., 1989. Alveolar macrophage–particle relationships during lung clearance. Am. J. Respir. Cell Mol. Biol. 1 (2), 145–154.
Li, Z., Potts-Kant, E.N., Garantziotis, S., Foster, W.M., Hollingsworth, J.W., 2011. Hyaluronan signaling during ozone-induced lung injury requires TLR4, MyD88, and TIRAP. PLoS One 6 (11), e27137.
Maes, T., Bracke, K.R., Vermaelen, K.Y., Demedts, I.K., Joos, G.F., Pauwels, R.A., Brusselle, G.G., 2006. Murine TLR4 is implicated in cigarette smoke-induced pulmonary inflammation. Int. Arch. Allergy Immunol. 141 (4), 354–368.
Ma-Hock, L., Treumann, S., Strauss, V., Brill, S., Luizi, F., Mertler, M., Wiench, K., Gamer, A.O., Ravenzwaay, B., Landsiedel, R., 2009. Inhalation toxicity of multi-wall carbon nanotubes in rats exposed for 3 months. Toxicol. Sci. kfp146.
Marshall, B.G., Wangoo, A., Cook, H.T., Shaw, R.J., 1996. Increased inflammatory cytokines and new collagen formation in cutaneous tuberculosis and sarcoidosis. Thorax 51 (12), 1253–1261.
Mercer, R.R., Hubbs, A.F., Scabilloni, J.F., Wang, L., Battelli, L.A., Friend, S., Castranova, V., Porter, D.W., 2011. Pulmonary fibrotic response to aspiration of multi-walled carbon nanotubes. Part. Fibre Toxicol. 8 (1), 21.
Muller, J., Huaux, F., Fonseca, A., Nagy, J.B., Moreau, N., Delos, M., Raymundo-Pimero, E., Beguin, F., Kirsch-Volders, M., Fenoglio, I., Fubini, B., Lison, D., 2008. Structural defects play a major role in the acute lung toxicity of multiwall carbon nanotubes: toxicological aspects. Chem. Res. Toxicol. 21 (9), 1698–1705.
Nygaard, U.C., Hansen, J.S., Samuelsen, M., Alberg, T., Marioara, C.D., Løvik, M., 2009. Single-walled and multi-walled carbon nanotubes promote allergic immune responses in mice. Toxicol. Sci. kfp057.
Oberdörster, G., Ferin, J., Gelein, R., Soderholm, S.C., Finkelstein, J., 1992. Role of the alveolar macrophage in lung injury: studies with ultrafine particles. Environ. Health Perspect. 97, 193.
Palomäki, J., Välimäki, E., Sund, J., Vippola, M., Clausen, P.A., Jensen, K.A., Savolainen, K., Matikainen, S., Alenius, H., 2011. Long, needle-like carbon nanotubes and asbestos activate the NLRP3 inflammasome through a similar mechanism. ACS Nano 5 (9), 6861–6870.
Porter, D.W., Hubbs, A.F., Mercer, R.R., Wu, N., Wolfarth, M.G., Sriram, K., Leonard, S., Battelli, L., Schwegler-Berry, D., Friend, S., Andrew, M., Chen, B.T., Tsuruoka, S., Endo, M., Castranova, V., 2010. Mouse pulmonary dose-and time course-responses induced by exposure to multi-walled carbon nanotubes. Toxicology 269 (2), 136–147.
Pulskamp, K., Diabaté, S., Krug, H.F., 2007. Carbon nanotubes show no sign of acute toxicity but induce intracellular reactive oxygen species in dependence on contaminants. Toxicol. Lett. 168 (1), 58–74.
Shaulian, E., Karin, M., 2002. AP-1 as a regulator of cell life and death. Nat. Cell Biol. 4 (5), E131–E136.
Tate, M.D., Pickett, D.L., van Rooijen, N., Brooks, A.G., Reading, P.C., 2010. Critical role of airway macrophages in modulating disease severity during influenza virus infection of mice. J. Virol. 84 (15), 7569–7580.
Thepen, T., Van Rooijen, N., Kraal, G., 1989. Alveolar macrophage elimination in vivo is associated with an increase in pulmonary immune response in mice. J. Exp. Med. 170 (2), 499–509.
Trinchieri, G., Sher, A., 2007. Cooperation of Toll-like receptor signals in innate immune defence. Nat. Rev. Immunol. 7 (3), 179–190.
Uto, T., Akagi, T., Yoshinaga, K., Toyama, M., Akashi, M., Baba, M., 2011. The induction of innate and adaptive immunity by biodegradable poly (γ-glutamic acid) nanoparticles via a TLR4 and MyD88 signaling pathway. Biomaterials 32 (22), 5206–5212.
Wang, L.H., Rothberg, K.G., Anderson, R.G., 1993. Mis-assembly of clathrin lattices on endosomes reveals a regulatory switch for coated pit formation. J. Cell Biol. 123 (5), 1107–1117.
Wang, X., Katwa, P., Podila, R., Chen, P., Ke, P.C., Rao, A.M., Walters, D.M., Wingard, C.J., Brown, J.M., 2011. Multi-walled carbon nanotube instillation impairs pulmonary function in C57BL/6 mice. Part. Fibre Toxicol. 8 (1), 24.
Ware, L.B., 2006. Pathophysiology of acute lung injury and the acute respiratory distress syndrome. Seminars in Respiratory and Critical Care Medicine vol. 27, No. 4. Thieme Medical Publishers, New York, NY, pp. 337–349 (August).
Zhao, M., Fernandez, L.G., Doctor, A., Sharma, A.K., Zarbock, A., Tribble, C.G., Kron, I.L., Laubach, V.E., 2006. Alveolar macrophage activation is a key initiation signal for acute lung ischemia–reperfusion injury. Am. J. Physiol. Lung Cell. Mol. Physiol. 291 (5), L1018–L1026.